

## **Thermophoresis and Dufour-Soret Contributions to MHD Free Convective Heat and Mass Transfer in Micropolar Fluids with Variable Viscosity over an Inclined Quadratic Stretching Sheet**

*Mohammed Abdur Rahman*

Department of Mathematics, National University Bangladesh  
Gazipur-1704, Bangladesh  
E-mail: [abdur.rahman1@nu.ac.bd](mailto:abdur.rahman1@nu.ac.bd)

*Received 25 March 2025; accepted 12 May 2025*

**Abstract.** This study investigates the impact of thermophoresis and Dufour-Soret effects on magnetohydrodynamic (MHD) free convection steady-state flow of micropolar fluids flowing over a vertically inclined quadratic stretching sheet. The analysis combines the influence of suction, variable viscosity, and power-law temperature variations at the surface of the sheet in heat and mass transfer. The governing non-linear partial differential equations (PDEs) of fluid flow are converted into dimensionless ordinary differential equations (ODEs) employing suitable similarity transformation. Subsequently, the resulting similarity equations namely linear momentum, angular momentum, energy, and species continuity are solved numerically by applying Runge-Kutta sixth-order with Nachtsheim-Swigert shooting iteration technique accompanied by FORTRAN programming. The numerical results include velocity, micro-rotation, temperature, concentration profiles, and thermo-physical quantities such as Skin-friction coefficient, surface couple stress, Nusselt number, and Sherwood number for various governing prominent physical parameters. It is observed that with the increase of the magnetic field parameter  $M$  (0.01-0.04), the local skin-friction coefficient, local surface couple stress, local Nusselt number, and the local Sherwood number all decrease by approximately 0.33%, 0.35%, 0.0124%, and 0.0035% respectively. The Schmidt number  $Sc$  (0.33-1.0) is observed to increase approximately 0.109% in the local skin-friction coefficient, 0.946% in the local surface couple stress, 18.12% in the local Nusselt number, and 217.75% in the local Sherwood number. The numerical results are compared with previous research findings to ensure the exactness of the investigation. The findings reveal significant insights into industrial applications in micropolar fluids such as manufacturing stretched sheet, and material processing.

**Keywords:** Thermophoresis; Dufour effects; Soret effects; Quadratic stretching Sheet

**AMS Mathematics Subject Classification (2010):** 76E25

## 1. Introduction

The study of micropolar fluid flow over a non-linear stretching sheet provides valuable insights into complex fluid behavior by capturing minor rotational effects. This understanding helps us to analyze heat transfer and stress distributions more effectively. This knowledge is crucial in several practical fields of science and various industrial applications such as polymer extrusion in manufacturing [1], thermal insulation, fluid flowing in the brain, exotic lubricants, chemical catalytic reactors, oil exploration, colloidal expansions, and complexes, etc. [2,3]. Tripathy et al. conducted numerical learning of MHD micropolar fluid flow over a stretching sheet embedded beneath a porous surface using a chemical reaction and an irregular heat source [4]. A mathematical report on unstable 2D electromagnetic free convection micropolar fluid flow through an upward leaky plate and a porous medium was completed by Islam et al. [5]. Haque [6] examined the induced magnetic field on MHD micropolar fluid motion and transient heat-mass transportation entirely. Guedri et al. [7] investigated an extensible sheet with an incompressible two-dimensional micropolar fluid flow. Buzuzi et al. [8] studied how heat generation, radiation, and chemical reactions work in micropolar fluid with tiny particles flowing over an inclined surface. Micropolar fluid investigation on a continuous porous surface with the effect of inclined angle and Lorentz force on convective thermal-material transmission was performed by Hossain et al. [9]. Hasanuzzaman et al. [10] inquired into MHD conductive heat and mass transference affected by radiative and viscous dissipation over a vertical porous sheet. A numerical analysis of the MHD micropolar nanofluid flow over a vertically elongating sheet containing gyrotactic microorganisms with temperature-dependent viscosity was presented by Fatunmbi et al. [11]. The MHD field effect on steady or unsteady flow in porous or non-porous medium was recently observed by Hossain et al. [12].

Thermophoresis is a process where small particles like dust in a gas move from a hotter area to a cooler one due to temperature gradients. This happens because gas molecules collide with the particle differently on its hot and cold sides, creating a force that pushes particles toward the cooler area. For instance, if a cold surface is placed in a hot gas with particles, these particles can stick to the cold surface. This effect is useful in various applications, including removing dust from gas streams, analyzing exhaust particles from combustion, and studying particle deposition on turbine blades [13]. It is also crucial in manufacturing processes like creating ceramic powders, producing optical fibers, and improving efficiency in particle filtration [14]. Thermophoresis plays a role in managing contaminants in gases and dealing with potential radioactive particles in nuclear reactors, highlighting its importance across different industries. Dawar et al. [15] examined the movement of a 2D micropolar fluid and looked at the influences of various factors like magnetic fields, chemical reactions, Joule heating, thermophoresis, and Brownian motion. Waini et al. [16] investigated the micropolar fluid flow over a moving flat plate covering hybrid nanoparticles with the considerable effect of thermophoresis particle deposition and viscous dissipation.

The Soret and Dufour numbers, which are dimensionless quantities, are the interactions between temperature and concentration gradients in mixtures in transference phenomena. The Soret effect, shown by the Soret number ( $Sr$ ), which is the ratio of thermal diffusivity to mass diffusivity, is how temperature changes affect concentration (Soret effect). Mass diffusion is quantified as a result of temperature gradients. On the other

## Thermophoresis and Dufour-Soret Contributions to MHD Free Convective Heat and Mass Transfer in Micropolar Fluids with Variable Viscosity over an Inclined Quadratic Stretching Sheet

hand, the Dufour number ( $Df$ ), which shows how concentration differences affect temperature circulation (Dufour effect) and represents the ratio of mass diffusion to thermal diffusion, acts on the effect of concentration gradients on thermal diffusion. These numbers help to describe the behavior of fluid mixtures under various thermodynamic conditions when taken as a whole. These numbers are significant in fields like environmental engineering, material science, and chemical engineering, where processes like evaporation, drying, and chemical reactions rely greatly on heat and mass transfer. When Soret and Dufour's effects were present, Reddy et al. looked into how thermophoresis affected the heat and mass transfer flow of a micropolar fluid over a stretching sheet. [17]. The Soret and Dufour effects on MHD micropolar fluid flow through a non-Darcy porous medium, where temperature and concentration vary non-linearly in the boundary layer region and diverge linearly with distance from the origin, were discussed by Reddy et al. [18]. The effects of heat and mass transfer, viscous dissipation, Joule heating, a heat sink, and radiation on MHD flow past a stretching surface were investigated by Verma et al. [19]. Borah et al. [20] investigated heat and mass transport phenomena associated with the MHD flow of micropolar fluid over a vertically stretched Riga plate by employing a uniform magnetic field applied parallel to the plate.

As indicated by the above literature survey and our limited knowledge, due to the inclined quadratic stretching sheet with power-law wall temperature along with suction effect in the presence of variable viscosity, there is no investigation available of different parameters like thermophoresis and Dufour-Soret number with their diverse values for free convective heat and mass transfer of MHD micropolar fluid flow problem. The numerical solutions for the non-dimensional equations such as velocity, microrotation, temperature, and concentration equations obtained are presented in graphical and tabular form to discuss their physical nature on heat and mass transfer flow. From the numerical computations, the local skin friction coefficient, local surface couple stress, heat transfer rate, and mass transfer rate are also calculated and presented in tabular form.

### 2. Physical modeling

This study considers a steady two-dimensional, viscous, incompressible, and electrically conducting convective heat and mass transfer of micropolar fluid flowing over a quadratic stretching sheet inclined at an acute angle  $\alpha$  from the vertical. The  $x$ -axis is aligned along the sheet, while the  $y$ -axis is determined perpendicular to the sheet.  $u$  and  $v$  indicate fluid velocities along the axes  $x$  and  $y$ , respectively. The stretching sheet velocity is assumed as  $u=ax^2$ , where  $a > 0$  is a constant, stretching rate. Suction/injection of the fluid  $v_w(x)$  is exerted normally on the stretching sheet, with suction represented by a negative value ( $< 0$ ) and injection by a positive value ( $> 0$ ). The uniform magnetic field strength  $B_0$  is applied perpendicular to the stretching sheet. Following the boundary layer analysis, the temperature gradient  $\left(\frac{\partial T}{\partial x}\right)$  across the surface of the sheet is much lower than the temperature gradient  $\left(\frac{\partial T}{\partial y}\right)$  normal to the surface of the sheet, that is,  $\frac{\partial T}{\partial y} \gg \frac{\partial T}{\partial x}$  [21]. The

## Mohammed Abdur Rahman

gravitational acceleration  $g_0$  acts downward in the opposite direction of the  $x$  coordinate. The analysis is carried out for the viscosity of the fluid depending on temperature defined as  $\mu = \mu_\infty \left( \frac{\theta_r}{\theta_r - \theta} \right)$  and the power-law variation of the wall temperature  $T_w(x) = T_\infty + Ax^p$  where  $T_w$  and  $T_\infty$  denote wall and free stream temperatures [22], [23]. This study's physical model is shown in Figure 1 below.

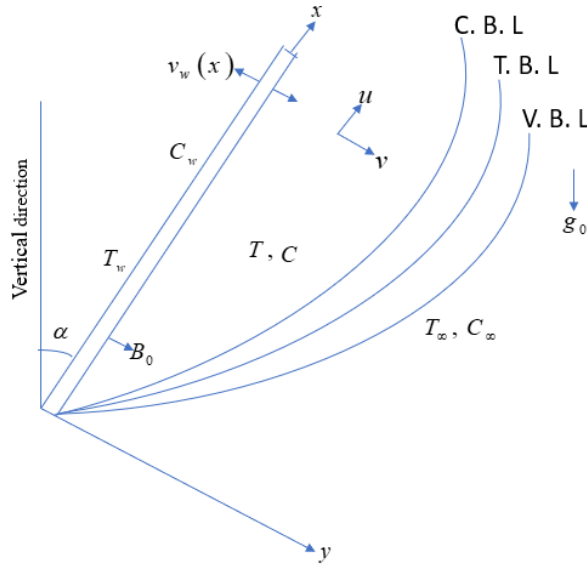


Figure 1: Flow configuration and coordinate system.

### 3. Mathematical modeling

Under the above assumptions together with Boussinesq's approximation the governing equations of heat and mass transfer with appropriate boundary conditions are considered as [24], [25]:

Equation of continuity:

$$\frac{\partial u}{\partial x} + \frac{\partial v}{\partial y} = 0, \quad \dots(1)$$

Equation of linear momentum:

$$u \frac{\partial u}{\partial x} + v \frac{\partial u}{\partial y} = \frac{\partial}{\partial y} \left( \nu_a \frac{\partial u}{\partial y} \right) + \frac{S}{\rho} \frac{\partial \sigma}{\partial y} + g_0 \beta (T - T_\infty) \cos \alpha + g_0 \beta^* (C - C_\infty) \cos \alpha - \frac{\sigma' B_0^2 u}{\rho}, \dots(2)$$

Equation of angular momentum:

$$u \frac{\partial \sigma}{\partial x} + v \frac{\partial \sigma}{\partial y} = \frac{\nu_s}{\rho j} \frac{\partial^2 \sigma}{\partial y^2} - \frac{S}{\rho j} \left( 2\sigma + \frac{\partial u}{\partial y} \right), \quad \dots(3)$$

Equation of energy:

$$u \frac{\partial T}{\partial x} + v \frac{\partial T}{\partial y} = \frac{k}{\rho c_p} \frac{\partial^2 T}{\partial y^2} + \frac{D_m k_T}{c_s c_p} \frac{\partial^2 C}{\partial y^2} + \frac{Q_0}{\rho c_p} (T - T_\infty), \quad \dots(4)$$

**Thermophoresis and Dufour-Soret Contributions to MHD Free Convective Heat and Mass Transfer in Micropolar Fluids with Variable Viscosity over an Inclined Quadratic Stretching Sheet**

Equation of species continuity:

$$u \frac{\partial C}{\partial x} + v \frac{\partial C}{\partial y} = \frac{D_m K_T}{T_m} \frac{\partial^2 T}{\partial y^2} + D_m \frac{\partial^2 C}{\partial y^2} - \frac{\partial}{\partial y} [V_T (C - C_\infty)], \quad \dots(5)$$

Boundary conditions:

$$u = ax^2, \quad v = v_w(x), \quad \sigma = -n \frac{\partial u}{\partial y}, \quad T_w(x) = T_\infty + Ax^p, \quad C = C_w \quad \text{for } y=0 \quad \dots(6)$$

$$u \rightarrow 0, \quad \sigma \rightarrow 0, \quad T \rightarrow T_\infty, \quad C \rightarrow C_\infty \quad \text{for } y \rightarrow \infty \quad \dots(7)$$

In the above equations and boundary conditions,  $\nu_a = \frac{\mu + S}{\rho}$  is the apparent kinematic viscosity,  $\mu$  is the fluid dynamic viscosity,  $S$  is the microrotation rate,  $\rho$  is the mass density of the fluid,  $\sigma$  is the microrotation component normal to the  $xy$ -plane,  $\beta$  is the volumetric expansion coefficient with temperature,  $T$  is the temperature of the fluid,  $\alpha$  is the angle of inclination to the vertical direction,  $\beta^*$  is the volumetric expansion coefficient with concentration,  $C$  is the concentration of the fluid,  $C_\infty$  is the free stream concentration,  $\sigma'$  is the electrical conductivity,  $\nu_s = \left( \mu + \frac{S}{2} \right) j$  is the spin-gradient viscosity [26, 27],  $j$  is the micro-inertia density,  $k$  is the thermal conductivity of the fluid,  $c_p$  is the specific heat of the fluid at constant pressure,  $D_m$  is the mass diffusivity coefficient,  $k_T$  is the thermal diffusion ratio,  $c_s$  is the concentration susceptibility,  $Q_0$  is the dimensional heat generation or absorption coefficient,  $T_m$  is the fluid mean temperature,  $V_T = -\frac{k_t \nu_\infty}{T_r} \frac{\partial T}{\partial y}$  is the thermophoretic deposition velocity,  $k_t$  is the thermophoretic coefficient,  $T_r$  is some reference temperature,  $n$  is the microrotation parameter,  $A$  is a positive constant, and  $p$  is the wall temperature index. The kinematic viscosity of an ambient fluid is denoted by  $\nu_\infty = \frac{\mu_\infty}{\rho}$  where  $\mu_\infty$  is the dynamic viscosity at ambient temperature.

It should be mentioned that  $v_w(x)=0$  corresponds to an impermeable sheet and  $p=0$  represents the constant temperature of the fluid at the surface of the sheet. The value  $n=0$  indicates strong concentration and represents concentrated particles flowing closest to the wall surface that cannot translate or rotate [28], [29]. The case  $n=0.5$  represents weak concentration and the fluid behaves like an ordinary (Newtonian) viscous flow [30]. For  $n=1$ , this value signifies the turbulent boundary layer flows [31].

Lai and Kulacki [32] assumed that the fluid dynamic viscosity varies inversely as a linear function of temperature denoted as

Mohammed Abdur Rahman

$$\frac{1}{\mu} = \frac{1}{\mu_\infty} [1 + \delta(T - T_\infty)], \quad \dots(8)$$

where  $\delta$  represents the thermal property of liquid. Equation (8) can be re-written as

$$\frac{1}{\mu} = b(T - T_r), \quad \dots(9)$$

where  $b = \frac{\delta}{\mu_\infty}$  and  $T_r = T_\infty - \frac{1}{\delta}$  are constants and define the dimensionless values as a function of reference state and thermal property of liquid.

The dimensionless form of temperature

$$\theta = \frac{T - T_\infty}{T_\infty - T_w} + \theta_r, \quad \dots(10)$$

and the variable viscosity parameter  $\theta_r = \frac{T_r - T_\infty}{T_w - T_\infty}, \quad \dots(11)$

The value of  $\theta_r$  is large, with  $T_w - T_\infty$  is a small and minor value of  $\theta_r$  implies a significant operating temperature difference. Equations (8), and (10) are used to get the following relation:

$$\mu = \mu_\infty \left( \frac{\theta_r}{\theta_r - \theta} \right), \quad \dots(12)$$

It is observed that  $\theta_r$  cannot take a value between 0 and 1 and the value of  $\theta_r$  is negative for liquids whereas  $\theta_r > 1$  is constrained for gases.

The thermophoretic parameter  $\tau$  is defined as follows (Mills et al. [33], and Tsai [34]):

$$\tau = -\frac{k_t(T_w - T_\infty)}{T_r}, \quad \dots(13)$$

where  $\tau > 0$  indicates the surface of the sheet is cold whereas  $\tau < 0$  shows a hot surface sheet. The sheet surface of the present problem is considered cold.

We introduce the following appropriate similarity variables:

$$\left. \begin{aligned} u = \frac{\partial \psi}{\partial y}, v = -\frac{\partial \psi}{\partial x}, \eta = y \sqrt{\frac{ax}{\nu_\infty}}, \psi = \sqrt{av_\infty} x^{\frac{3}{2}} f(\eta), \\ \sigma = \sqrt{\frac{a^3}{\nu_\infty}} x^{\frac{5}{2}} g(\eta), \theta(\eta) = \frac{T - T_\infty}{T_w - T_\infty}, \phi(\eta) = \frac{C - C_\infty}{C_w - C_\infty} \end{aligned} \right\}, \quad \dots(14)$$

where  $\psi = \psi(x, y)$  is the stream function and  $f$  is the dimensionless stream function.

**Thermophoresis and Dufour-Soret Contributions to MHD Free Convective Heat and Mass Transfer in Micropolar Fluids with Variable Viscosity over an Inclined Quadratic Stretching Sheet**

The converted coupled nonlinear ordinary differential equations of the given governing equations (1)-(5) obtained by using transformation equations (14) are given as follows:

$$\left(\frac{\theta_r}{\theta_r - \theta} + \Delta\right) f''' + \frac{3}{2} f f'' - 2 f'^2 + \frac{\theta_r}{(\theta_r - \theta)^2} f'' \theta' + \Delta g' + (Gr\theta + Gm\varphi) \cos \alpha - Mf' = 0, \quad (15)$$

$$\left(\frac{\theta_r}{\theta_r - \theta} + \frac{1}{2} \Delta\right) \xi g'' - \Delta(2g + f'') - \xi \left(\frac{5}{2} f' g - \frac{3}{2} f g'\right) = 0, \quad \dots(16)$$

$$\theta'' + Pr \left(1 - \frac{\theta}{\theta_r}\right) \left(\frac{3}{2} f \theta' - p f' \theta + Q \theta + Df \varphi''\right) = 0, \quad \dots(17)$$

$$\varphi'' + Sc \left(1 - \frac{\theta}{\theta_r}\right) \left(\frac{3}{2} f - \tau \theta'\right) \varphi' - Sc \left(1 - \frac{\theta}{\theta_r}\right) \tau \theta'' \varphi + Sc \left(1 - \frac{\theta}{\theta_r}\right) Sr \theta'' = 0, \quad \dots(18)$$

where  $\Delta = \frac{S}{\mu_\infty}$  is the vortex viscosity parameter,  $Gr = \frac{g_0 \beta (T_w - T_\infty)}{a^2 x^3}$  is the local Grashof

number,  $Gm = \frac{g_0 \beta^* (C_w - C_\infty)}{a^2 x^3}$  is the modified local Grashof number,  $M = \frac{\sigma' B_0^2}{\rho a x}$  is the

magnetic field parameter,  $\xi = \frac{j a x}{\nu_\infty}$  is the local micro-inertia density parameter,

$Pr = \left(\frac{\theta_r}{\theta_r - \theta}\right) \frac{\mu_\infty c_p}{k}$  is the Prandtl number,  $Q = \frac{Q_0}{\rho c_p a x}$  is the local heat generation /

absorption parameter,  $Df = \frac{D_m k_T (C_w - C_\infty)}{c_s c_p \nu_\infty (T_w - T_\infty)}$  is the Dufour number,  $Sc = \left(\frac{\theta_r}{\theta_r - \theta}\right) \frac{\nu_\infty}{D_m}$  is

the Schmidt number,  $Sr = \frac{D_m k_T (T_w - T_\infty)}{\nu_\infty T_m (C_w - C_\infty)}$  is the Soret number and primes symbolize

differentiation for similarity variable  $\eta$ .

The boundary conditions (6)-(7) altered as follows:

$$f = f_w, f' = 1, g = -n f''(0), \theta = 1, \varphi = 1 \text{ for } \eta = 0, \quad \dots(19)$$

$$f' = 0, g = 0, \theta = 0, \varphi = 0 \text{ for } \eta \rightarrow \infty, \quad \dots(20)$$

where  $f_w = -\frac{2\nu_w(x)}{3\sqrt{a\nu_\infty x}}$  is the suction/injection velocity at the sheet for  $f_w > 0$  and  $f_w < 0$ .

The parameters of engineering interest for the current problem are the local skin-friction coefficient, local surface couple stress, local Nusselt number, and the local Sherwood number defined by, respectively,

$$Cf_x \propto f''(0), M_x \propto g'(0), Nu_x \propto -\theta'(0), \text{ and } Sh_x \propto -\varphi'(0) \quad \dots(21)$$

**4. Method of numerical solution and validation**

The transformed system of non-linear ordinary differential equations (15)-(18) together with the boundary conditions (19)-(20) have been solved numerically by utilizing the shooting iteration technique suggested by Nachtsheim-Swigert [35] along with the sixth-order Runge integration scheme. Various groups of the arisen parameters were considered in different phases.

**Table 1.** Comparison of the local Stanton number obtained in the present work and those obtained by Tsai [34] and Alam [36].

$\tau$	$f_w$	Tsai [34]	Alam [36]	Present study
0.1	1.0	0.7346	0.7273	0.7334
0.1	0.5	0.3810	0.3724	0.3701
0.1	0.0	0.0275	0.0273	0.0274
1.0	1.0	0.9134	0.8929	0.9024
1.0	0.5	0.5598	0.5580	0.5588
1.0	0.0	0.2063	0.2060	0.2062

A step size of  $\Delta\eta=0.01$  was selected in all the computations that satisfied a convergent criterion of  $10^{-6}$  in all cases. To see the accuracy of the present numerical method, we have compared our results with those of [34] and [36]. Thus, Table 1 compares the local Stanton number obtained in the present work with those obtained by [34] and [36]. Excellent agreement exists among the results, which leads to confidence in the present numerical method.

**5. Results and discussion**

The results of the numerical computations based on the earlier stated method are displayed graphically in Figures 2-9 and Tables 2-5 for prescribed parameters. In the calculation, we have used  $Pr = 0.70$  (air),  $Sc = 0.22$  (hydrogen),  $Gr = 10$ , and  $Gm = 4$  (free convection). The solution of each parameter originated in the problem has been found for a set of different values keeping the value of other parameters unchanged.

**5.1. Role of vortex viscosity**

The effect of vortex viscosity parameter  $\Delta$  on the dimensionless velocity and microrotation profiles is shown in Figure 2(a)-(b), respectively.

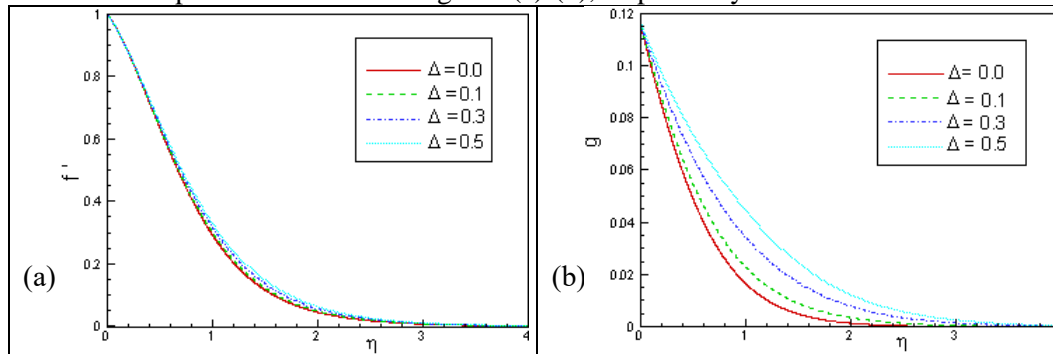


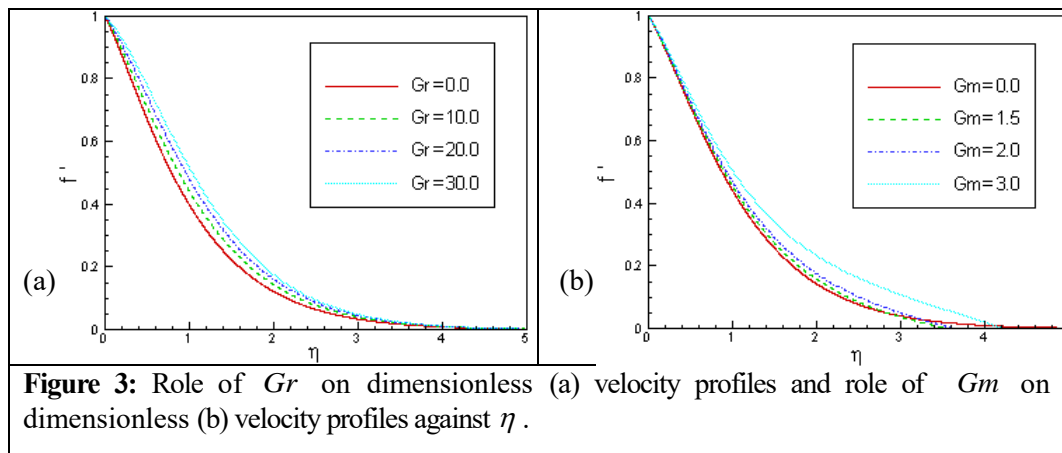
**Figure 2:** Role of  $\Delta$  on dimensionless (a) velocity, (b) microrotation profiles against  $\eta$  .

## Thermophoresis and Dufour-Soret Contributions to MHD Free Convective Heat and Mass Transfer in Micropolar Fluids with Variable Viscosity over an Inclined Quadratic Stretching Sheet

It is seen from Figure 2(a)-(b) that as vortex viscosity parameter values increase both the velocity and microrotation profiles increase. Velocity increases because with the increasing values of  $\Delta$  the viscosity decreases. It is also interesting to note that the effect of microrotation is prominently higher as the values of  $\Delta$  are growing. Vortex viscosity impacts fluid velocity and microrotation, which can be used in newer technologies such as advanced mixing systems or enhanced cooling methods in the manufacturing and power industries.

### 5.2. Role of local Grashof number and modified local Grashof number

Figures 3(a)-(b), respectively display the velocity profiles for several values of the local Grashof number  $Gr$  and modified local Grashof number  $Gm$ . The magnitude of both  $Gr$  and  $Gm$  indicate whether the flow is laminar or turbulent. Typically, low  $Gr$  or  $Gm$  indicates laminar flow whereas high  $Gr$  or  $Gm$  indicates turbulent flow.



Increasing effects on velocity profiles are found for both  $Gr$  and  $Gm$  with their increasing values as observed in Figures 3(a)-(b). It is to be discovered that the velocity profiles of the fluid accelerate with more significant amounts of  $Gr$ , and  $Gm$ . Here, positive values of  $Gr$  means the system is heating.  $Gr > 0$  suggests that buoyancy encourages upward movement in the fluid, while  $Gm > 0$  indicates active mass or momentum transfer improves mixing and flow dynamics.

### 5.3. Role of angle of inclination

Representative velocity, microrotation, temperature, and concentration profiles for four typical angles of inclination ( $\alpha = 0^\circ, 10^\circ, 20^\circ$ , and  $30^\circ$ ) are presented in Figures 4(a)-(d), respectively. It is revealed from Figure 4(a) that increasing the angle of inclination decreases the velocity inside the hydrodynamic boundary layer. The fact is that, as the angle of inclination increases, the effect of the buoyancy force due to thermal diffusion decreases by a factor of  $\cos\alpha$ . Consequently, the driving force to the fluid decreases; as a result, velocity profiles decrease. From Figures 4(b)-(d) we observe that microrotation, thermal, and concentration boundary layer thickness increase as the angle of inclination increases.

The increasing effect of  $\alpha$  on the concentration boundary layer is more potent than other boundary layers.

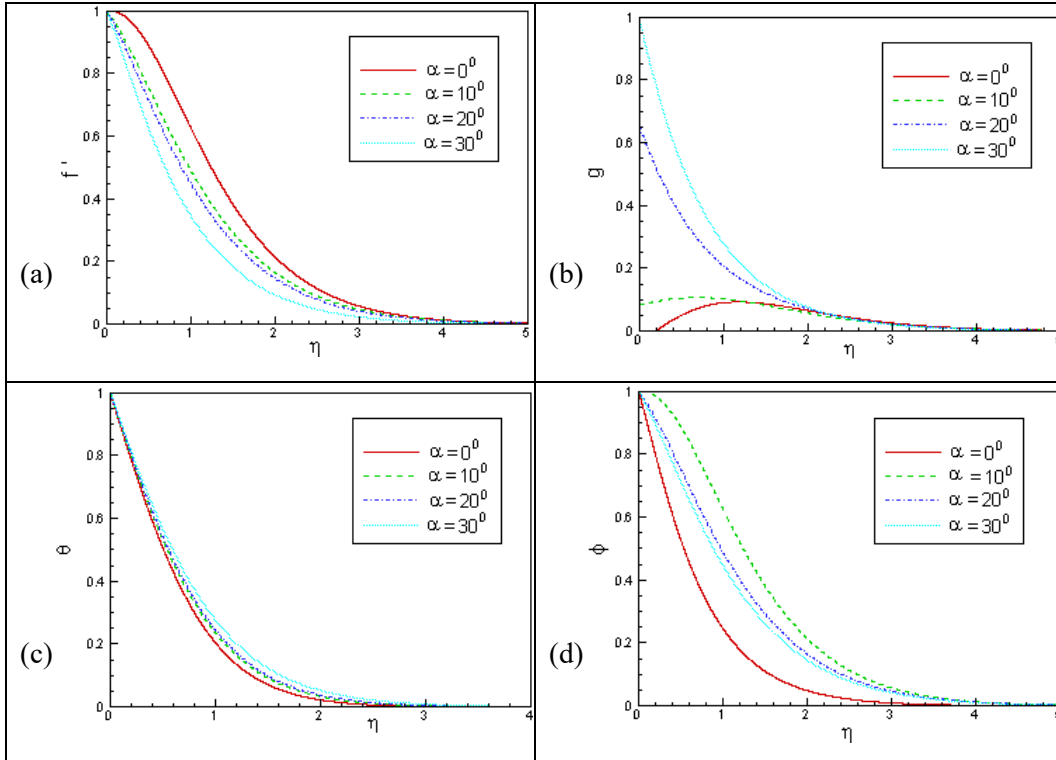


**Figure 4:** Role of  $\alpha$  on dimensionless (a) velocity, (b) microrotation, (c) temperature, and (d) concentration profiles against  $\eta$ .

#### 5.4. Role of magnetic field parameter

Figures 5(a)-(d) display the effect of the magnetic field parameter  $M$  on the velocity, microrotation, temperature, and concentration profiles respectively. The presence of a magnetic field normal to the flow in an electrically conducting fluid introduces a Lorentz force that acts against the flow. This resistive force tends to slow down the flow; hence, the magnitude of fluid velocity reduces in the boundary layer with the increase of the magnetic field parameter as observed in Figure 5(a).

**Thermophoresis and Dufour-Soret Contributions to MHD Free Convective Heat and Mass Transfer in Micropolar Fluids with Variable Viscosity over an Inclined Quadratic Stretching Sheet**

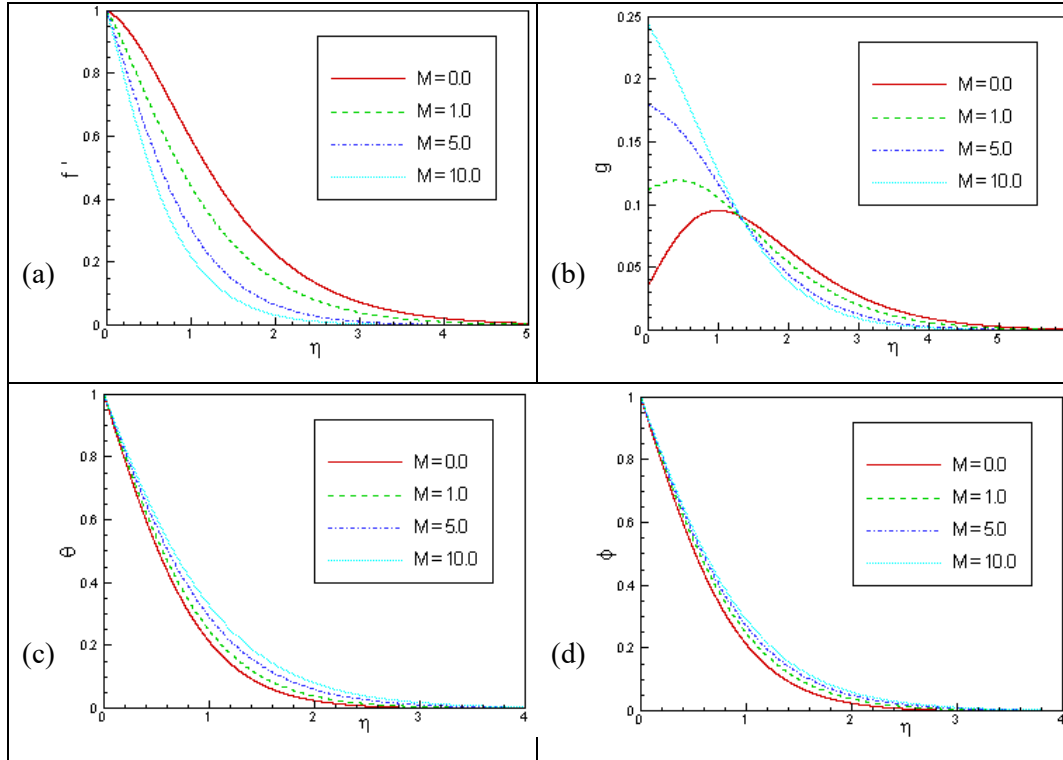
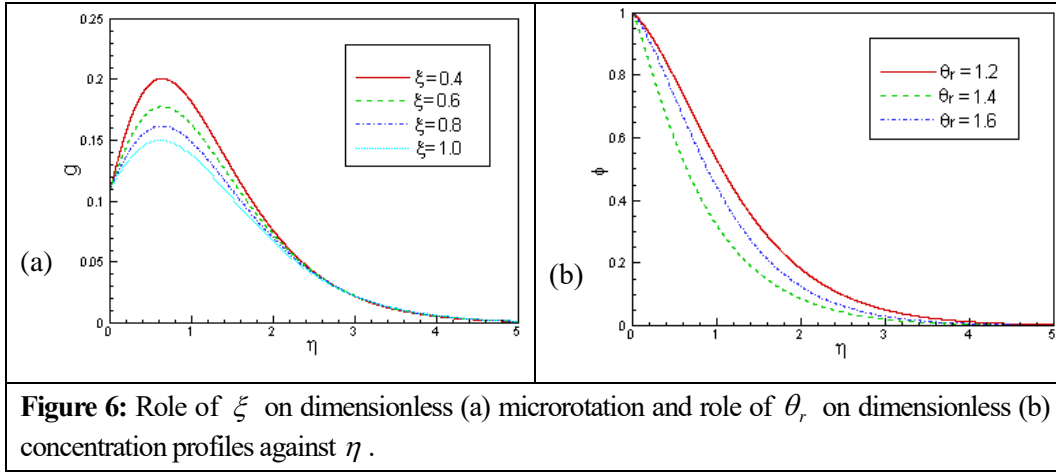


**Figure 5:** Role of  $M$  on dimensionless (a) velocity, (b) micro-rotation, (c) temperature, and (d) concentration profiles against  $\eta$ .

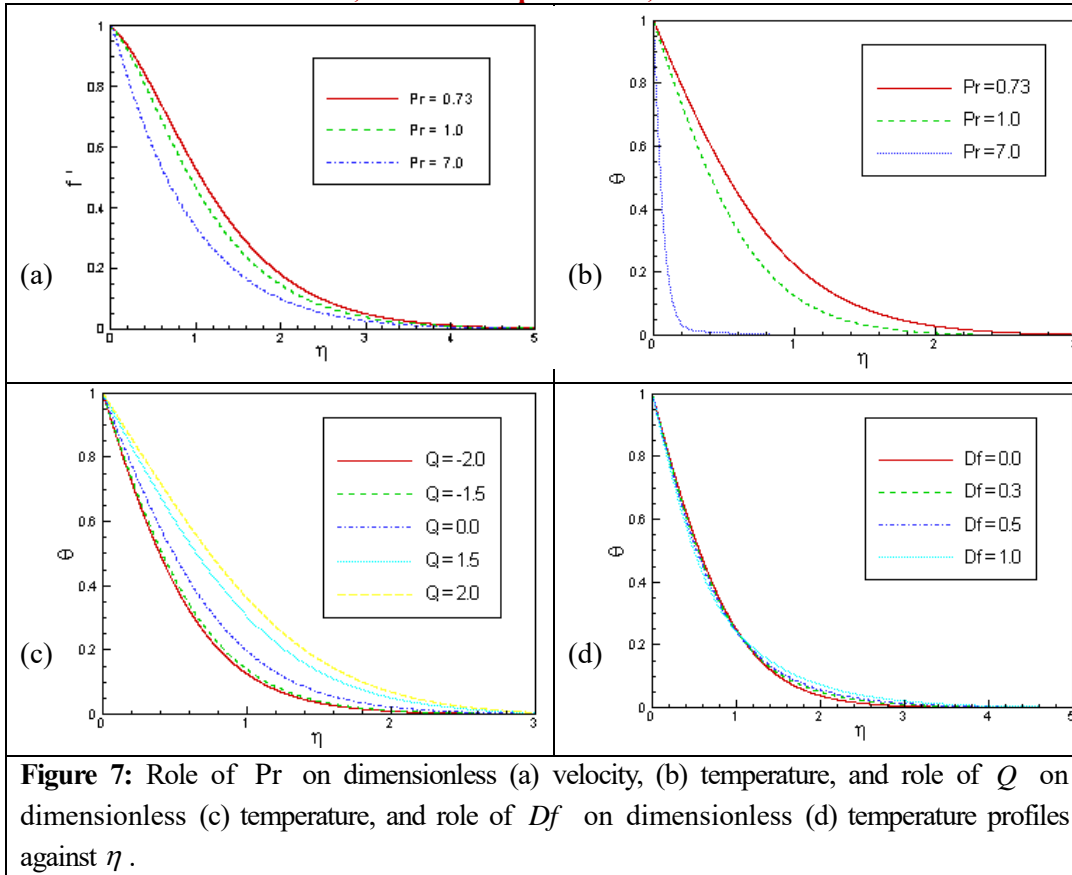
The effects of  $M$  on the microrotation profiles are presented in Figure 5(b) that with the increase of  $M$  microrotation increases near the surface and decreases far away from the surface. It is also seen from Figure 5(c) that the thickness of the thermal boundary layer and the temperature in the boundary layer rises with the increase of the magnetic field parameter. It can be seen in Figure 5(d) that the increased magnetic field parameter  $M$  increases the magnitude of concentration profiles.

**5.5. Role of local micro-inertia density parameter, and variable viscosity**

It is seen from Figure 6(a) that the microrotation decreases with the increase in the local micro-inertia density parameter  $\xi$ . It is evident because the higher local micro-inertia density parameter exerts more resistance to reducing microrotation in fluid particles relative to the flow field. Concentration profiles decrease as variable viscosity parameter  $\theta_r$  is increased as seen in Figure 6(b). Also, it is observed that with the fixed values of gases, the concentration profile decreases as  $\eta$  increases.



### 5.6. Role of Prandtl number, heat source parameter, and Dufour number



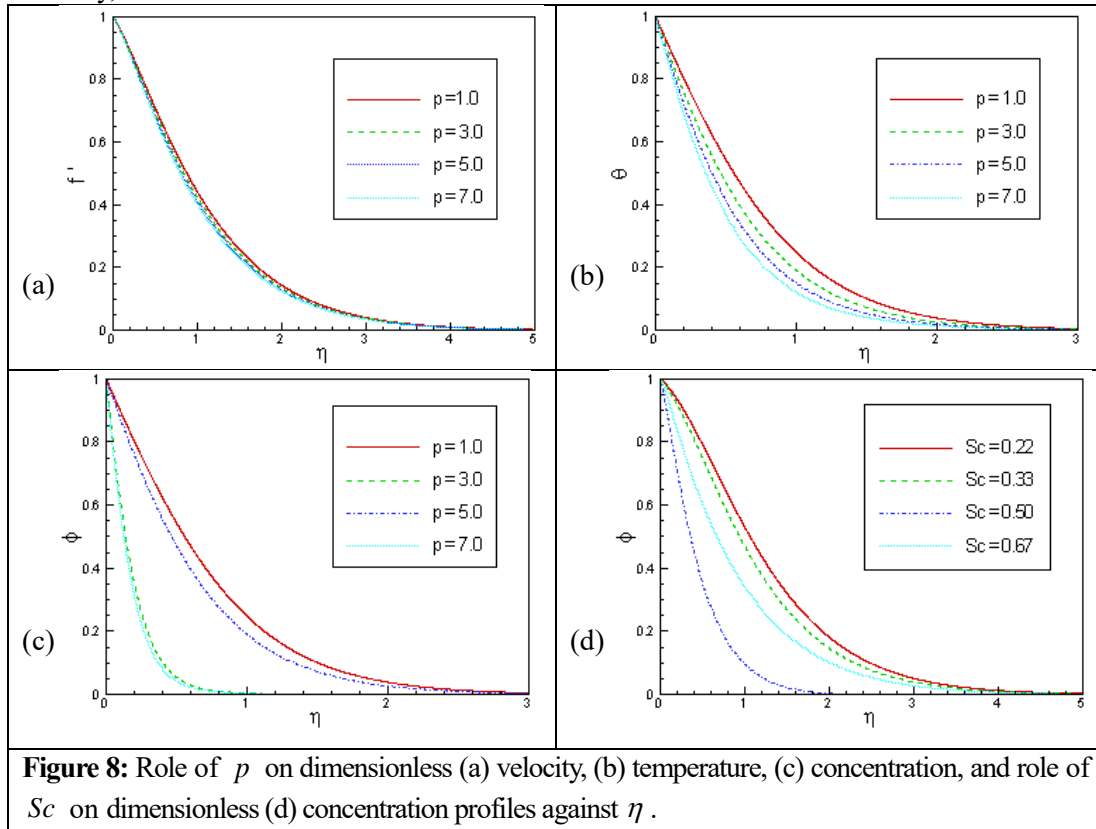
Figures 7(a)-(b), respectively show the effect of various Prandtl number Pr on velocity and temperature profiles. From here, we see that both the velocity and temperature profiles decline significantly with the rise of different values of Pr for air, water, and oil

**Thermophoresis and Dufour-Soret Contributions to MHD Free Convective Heat and Mass Transfer in Micropolar Fluids with Variable Viscosity over an Inclined Quadratic Stretching Sheet**

respectively. It is evident from Figure 7(c) that temperature profiles increase broadly with the increase of heat source parameter  $Q$  representing physical cooling, thermal equilibrium, and heating for its different state of values while Figure 7(d) reveals that temperature profiles increase minimally with different escalated Dufour number  $Df$ .

**5.7. Role of wall temperature index, and Schmidt number**

An increase in the wall temperature index  $p$  results in higher viscosity, which consequently leads to simultaneous reductions in the fluid velocity, temperature, and concentration, as demonstrated in Figure 8(a)-(c). Figure 8(d) illustrates the variation of concentration distribution of the flow field for different values of Schmidt number  $Sc$ . A higher value of  $Sc$  is associated with a lower concentration profile, as it signifies higher viscosity, which slows diffusion and reduces concentration variations.



**5.8. Role of Soret number, and thermophoretic parameter**

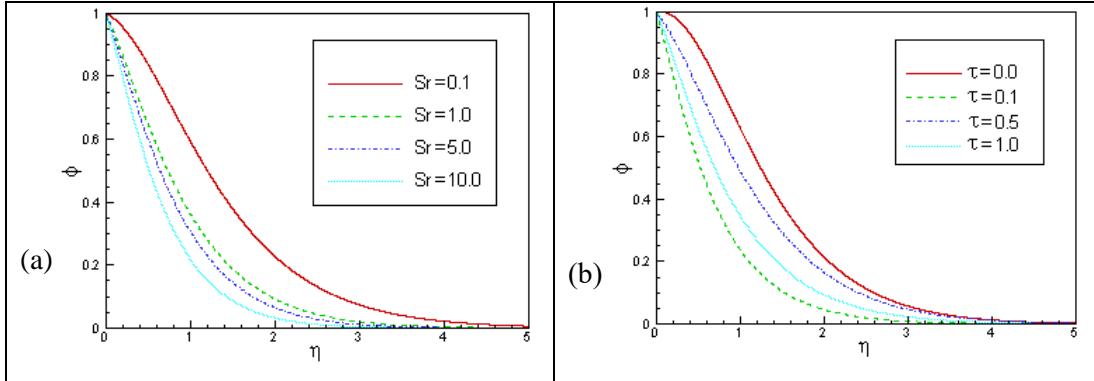


**Figure 9:** Role of  $Sr$  on dimensionless (a) concentration, and role of  $\tau$  on dimensionless (b) concentration profiles against  $\eta$ .

The influence of Soret number  $Sr$  and thermophoretic parameter  $\tau$  on the concentration profiles are shown in Figure 9(a) and 9(b) respectively. It is revealed from Figure 9(a) that increasing the positive value of  $Sr$  decreases the concentration. The fact is that, as the Soret number increases, stronger temperature variations lead to increased particle separation, which results in a lower concentration. It is observed from Figure 9(b) that an increase in  $\tau$  leads to a substantial decrease in the concentration.

**Table 2.** Effects of different values of  $M$  on  $f''(0)$ ,  $g'(0)$ ,  $-\theta'(0)$  and  $-\varphi'(0)$ .

$M$	$f''(0)$	$g'(0)$	$-\theta'(0)$	$-\varphi'(0)$
0.01	-1.15041970	-0.65831973	4.98579211	31.91141065
0.02	-1.15169398	-0.65908877	4.98558657	31.91104645
0.03	-1.15296964	-0.65985828	4.98538041	31.91067948
0.04	-1.15423861	-0.66062453	4.98517453	31.91030602

**Table 3.** Effects of different values of  $Sc$  on  $f''(0)$ ,  $g'(0)$ ,  $-\theta'(0)$  and  $-\varphi'(0)$ .

$Sc$	$f''(0)$	$g'(0)$	$-\theta'(0)$	$-\varphi'(0)$
0.33	-1.26694766	-0.73562996	4.20372687	10.03404138
0.67	-1.26667785	-0.73093883	4.58407761	20.71460550
0.75	-1.26623976	-0.73018252	4.67574097	23.33931929
1.0	-1.26556958	-0.72867066	4.96512552	31.85897572

**Table 4.** Effects of different values of  $\theta_r$  for both liquids and gases on  $-\theta'(0)$  and  $-\varphi'(0)$ .

$\theta_r$	$-\theta'(0)$	$-\varphi'(0)$
-5.0	49.08890398	616.55020421
-10.0	21.18091011	244.09786031
5.0	8.79687496	79.69272608
10.0	10.78551403	105.76854192

**Thermophoresis and Dufour-Soret Contributions to MHD Free Convective Heat and Mass Transfer in Micropolar Fluids with Variable Viscosity over an Inclined Quadratic Stretching Sheet**

**Table 5.** Effects of  $Df$ ,  $n$ ,  $Sr$ , and  $\alpha$  on the local Nusselt number ( $Nu_x$ ) for  $\Delta = 3.0$ ,  $Gr = 10.0$ ,  $Gm = 0.01$ ,  $M = 1.0$ ,  $\xi = 2.0$ ,  $Pr = 3.0$ ,  $Q = 0.5$ ,  $Sc = 1.0$ ,  $\theta_r = 1.6$ ,  $p = 1.0$ ,  $\tau = 0.8$ , and  $f_w = 1.0$ .

$Df$	$n$	$Sr$	$\alpha$	$Nu_x$
0.01	0	1.0	$0^0$	3.97556899
0.01	0.2	5.0	$30^0$	4.11414597
0.01	0.5	10.0	$60^0$	4.29534659
0.02	0	1.0	$0^0$	3.97556899
0.02	0.2	5.0	$30^0$	4.40667573
0.02	0.5	10.0	$60^0$	4.96512552
0.03	0	1.0	$0^0$	4.13521149
0.03	0.2	5.0	$30^0$	4.75325906
0.03	0.5	10.0	$60^0$	5.93909526

Tables 2-3, respectively, demonstrate the effects of the magnetic field parameter and Schmidt number, on the local skin-friction coefficient, local surface couple stress, local Nusselt number, and the local Sherwood number. Table 4 shows the effects of the variable viscosity parameter representing liquids and gases on the local Nusselt number and Sherwood number. Table 5 illustrates the effects of the Dufour number, microrotation parameter, Soret number, and inclination angle to vertical on the local Nusselt number. The trends of these parameters are self-evident from Tables 2-5; hence, they will not be discussed in detail to keep its brevity.

## 6. Conclusions

Effects of thermophoresis and Dufour-Soret to MHD free convective heat and mass transfer of a micropolar fluid with variable viscosity over an inclined quadratic stretching sheet have been studied. The significant observations of the study are made as follows:

1. As vortex viscosity parameter values grow high, both velocity and microrotation profiles rise, notably microrotation having a more prominent impact at higher values.
2. Both the Grashof number and the modified Grashof number increase the flow velocity due to the enhancement in the buoyancy force.
3. The higher the angle of inclination, the more sharply the reduction in velocity in the hydrodynamic boundary layer, while microrotation, thermal, and concentration boundary layer thicknesses grow. The effect on the concentration boundary layer is stronger than on the others.
4. A transverse magnetic field creates a Lorentz force that resists the flow, leading to a thermal and mass boundary layer thicker, and reducing the rate of heat and mass transfer. The increase in the value of magnetic field parameter microrotation increases near the surface but decreases further away.
5. The increase in the wall temperature index results in higher viscosity, consequently leading to simultaneous reductions in the fluid velocity, temperature, and concentration. This measure helps to increase the Nusselt and Sherwood numbers.

Mohammed Abdur Rahman

**Acknowledgements.** The author is grateful to the reviewers for their constructive comments for improvement of the paper.

**Author's Contributions.** This is a single author paper.

**Conflicts of interest.** The author declare that there is no conflicts of interest regarding the publication of this paper.

## REFERENCES

1. E.O.Fatunmbi, A.S.Oke and S.O.Salawu, Magnetohydrodynamic micropolar nanofluid flow over a vertically elongating sheet containing gyrotactic microorganisms with temperature-dependent viscosity, *Results in Materials*, 19 (2023) Online article 100453.
2. MD.Shamshuddin, T.Thirupathi and P.V.Satya Narayana, Micropolar fluid flow induced due to a stretching sheet with heat source/sink and surface heat flux boundary condition effect, *Journal of Applied and Computational Mechanics*, 5(5) (2019) 816-826.
3. A.Abbas, H.Ahmad, M.Mumtaz, A.Ilyas and M.Hussan, MHD dissipative micropolar fluid flow past stretching sheet with heat generation and slip effects, *Waves in Random and Complex Media*, (2022) Online article, 1-15.
4. R.S.Tripathy, G.C.Dash, S.R.Mishra and M.M.Hoque, Numerical analysis of hydromagnetic micropolar fluid along a stretching sheet embedded in porous medium with non-uniform heat source and chemical reaction, *Engineering Science and Technology, an International Journal*, 19(3)(2016) 1573-1581.
5. M.R.Islam, S.Nasrin and M.M.Alam, Unsteady electromagnetic free convection micropolar fluid flow through a porous medium along a vertical porous plate, *Open Journal of Applied Sciences*, 10(11), (2020) 701-718.
6. M.Haque, Heat and mass transfer analysis on magneto micropolar fluid flow with heat absorption in induced magnetic field, *Fluids*, 6(3) (2021) 126.
7. K.Guedri, N.A.Ahammad, S.Nadeem, E.M.Tag-ElDin, A.U.Awan and M.F. Yassen, Insight into the heat transfer of third-grade micropolar fluid over an exponentially stretched surface, *Scientific Reports*, 12(1) (2022) Online article 15577.
8. G.Buzuzi, A.N.Buzuzi, T.Nyamayaro and W.Manamela, The study of magneto hydrodynamic free convective flow and heat transfer in a porous medium with heat generation, radiation absorption and chemical reaction, *International Journal of Applied Mathematics*, 33(4), (2020) 733-756.
9. M.Hossain, M.M.T.Hossain and R.Nasrin, Time-dependent magneto-convective thermal-material transfer by micropolar binary mixture fluid passing a vertical surface, *Science and Technology Asia*, 28(1) (2023) 33-47.
10. M.Hasanuzzaman, S.Akter, S.Sharin, M.M.Hossain, A.Miyara and M.A.Hossain, Viscous dissipation effect on unsteady magneto-convective heat-mass transport passing in a vertical porous plate with thermal radiation, *Helvion*, 9(3), (2023) Online article 14207.
11. E.O.Fatunmbi, A.S.Oke, and S.O.Salawu, Magnetohydrodynamic micropolar nanofluid flow over a vertically elongating sheet containing gyrotactic microorganisms with temperature-dependent viscosity, *Results in Materials*, 19, (2023) Online article 100453.

**Thermophoresis and Dufour-Soret Contributions to MHD Free Convective Heat and Mass Transfer in Micropolar Fluids with Variable Viscosity over an Inclined Quadratic Stretching Sheet**

12. M.M.Hossain, R.Nasrin and M.Hasanuzzaman, Unsteady magneto porous convective transport by micropolar binary fluid due to inclined plate: An inclusive analogy, *Heliyon*, 20(2), (2024) Online article 24314.
13. H.M.Duwairi and R.A.Damseh, Effect of thermophoresis particle deposition on mixed convection from vertical surfaces embedded in saturated porous medium, *International Journal of Numerical Methods for Heat and Fluid Flow*, 18(2), (2008) 202-216.
14. M.S.Alam, M.M.Rahman and M.A.Sattar, Transient Magnetohydrodynamic Free Convective Heat and Mass Transfer Flow with Thermophoresis past a Radiate Inclined Permeable Plate in the Presence of Variable Chemical Reaction and Temperature Dependent Viscosity, *Nonlinear Analysis: Modelling and Control*, 14(1), (2009) 3-20.
15. A.Dawar, Z.Shah, A.Tassaddiq, S.Islam and P.Kumam, Joule heating in magnetohydrodynamic micropolar boundary layer flow past a stretching sheet with chemical reaction and microstructural slip, *Case Studies in Thermal Engineering*, 25, (2021) Online article 100870.
16. I.Waini, A.Zaib, A.Ishak and I.Pop, Thermophoresis particle deposition of  $\text{CoFe}_2\text{O}_4\text{-TiO}_2$  hybrid nanoparticles on micropolar flow through a moving flat plate with viscous dissipation effects, *International Journal of Numerical Methods for Heat and Fluid Flow*, 32(10), (2022) 3259-3282.
17. P.S.Reddy and A.J.Chamkha, Soret and Dufour effects on MHD heat and mass transfer flow of a micropolar fluid with thermophoresis particle deposition, *Journal of Naval Architecture and Marine Engineering*, 13, (2015) 39-50.
18. G.V.R.Reddy and Y.H.Krishna, Soret and Dufour effects on MHD micropolar fluid flow over a linearly stretching sheet, through a non-darcy porous medium, *International Journal of Applied Mechanics and Engineering*, 23(2), (2018) 485-502.
19. K.Verma and B.R. Sharma, Soret and Dufour effects on MHD flow with heat and mass transfer past an exponentially stretching sheet with viscous dissipation and joule heating, *Latin American Applied Research*, 52(2), (2022) 83-88.
20. K.Borah, J.J.Konch and S.Chakraborty, Soret and Dufour effects on MHD flow of a micropolar fluid past over a vertical riga plate, *Journal of Applied Mathematics and Computational Mechanics*, 22(3), 2023 5-18.
21. M.A.Rahman, M.A.Alim and M.J.Islam, Thermophoresis effect on MHD forced convection on a fluid over a continuous linear stretching sheet in present of heat generation and Power-law wall temperature, *Annals of Pure and Applied Mathematics*, 4(2), 2013 192-204.
22. M.A.Rahman and M.A.Alim, Variable viscosity and suction effects on heat and mass transfer flow of micropolar fluid over a linearly stretched sheet with thermophoresis, *National University Journal of Science*, 2(1) (2015) 113-129.
23. H.Chaudhary, D.Sunil and V.N.Mishra, Effects of variable viscosity and thermal conductivity on MHD flow due to the permeable moving plate, *Stochastic Modeling and Applications*, 25(2) (2021) 271-288.
24. U.Hani, M.Ali and M.S.Alam, MHD boundary layer micropolar fluid flow over a stretching wedge surface: Thermophoresis and Brownian motion effect, *Journal of Thermal Engineering*, 10(2) (2024) 330-349.

**Mohammed Abdur Rahman**

25. R.P.Sudarsana and A.J. Chamkha, Soret and Dufour effects on MHD heat and mass transfer flow of a micropolar fluid with thermophoresis particle deposition, *Journal of Naval Architecture and Marine Engineering*, 13 (2016) 1813-1825.
26. D.A.S.Rees and A.P.Bassom, The Blasius boundary-layer flow of a micropolar fluid, *International Journal of Engineering Science*, 34, (1966) 113-124.
27. G.Ahmadi, Self-similar solution of incompressible micropolar boundary layer flow over a semi-infinite plate, *International Journal of Engineering Science*, 14 ( 1976) 639-646.
28. S.K.Jena and M.N.Mathur, Similarity solution for laminar free convection flow of thermomicropolar fluid past a non-isothermal vertical flat plate, *International Journal of Engineering Science*, 19 (1981) 1431-1439.
29. R.S.R.Gorla, H.S. Takhar and A.Slaouti, Magneto hydrodynamic free convection boundary layer flow of a thermo micropolar fluid over a vertical plate, *International Journal of Engineering Science*, 36 (1998) 315-327.
30. G.Ahmadi, Self-similar solution of incompressible micropolar boundary layer flow over a semi-infinite plate, *International Journal of Engineering Science*, 14 (1976) 639-646.
31. J.Peddison and R.P.McNitt, Boundary layer theory for micropolar fluid, *Recent Advances in Engineering Science*, 5 (1970) 405-426.
32. F.C.Lai and F.A.Kulacki, The effect of variable viscosity on convective heat and mass transfer along a vertical surface in saturated porous medium, *International Journal of Heat and Mass Transfer*, 33 (1990) 1028-1031.
33. A.F.Mills, X.Hang and F.Ayazi, The effect of wall suction and thermophoresis on aerosol-particle deposition from a laminar boundary layer on a flat plate, *International Journal of Heat and Mass Transfer*, 27 (1984) 1110-1114.
34. R.A.Tsai, Simple approach for evaluating the effect of wall suction and thermophoresis on aerosol particle deposition from a laminar flow over a flat plate, *International Communications in Heat and Mass Transfer*, 26 (1999) 249-257.
35. P.R.Nachtsheim and P.Swigert, Satisfaction of the asymptotic boundary conditions in numerical solution of the system of non-linear equations of boundary layer type, (1965) *NASA TND-3004*.
36. M.S.Alam, Effect of thermophoresis on MHD free convective heat and mass transfer flow along an inclined stretching sheet under the influence of Dufour-Soret effects with variable wall temperature, *Thammasat International Journal of Science and Technology*, 21(3) (2016) 46-58.